EFFECT OF THICKNESS PROFILE AND FG FUNCTION ON ROTATING DISKS UNDER THERMAL AND MECHANICAL LOADING

M. Jabbari **M. Ghannad**

Mechanical Engineering Faculty
Shahrood University
Shahrood, Iran

M. Z. Nejad *

Mechanical Engineering Department
Yasouj University
Yasouj, Iran

ABSTRACT

In this paper, a thermoelastic analysis of rotating disks with different thickness profiles made of functionally graded materials (FGMs) subjected to internal pressure is presented. Material properties (except Poisson's ratio) and disk thickness profile are described by means of two functions namely power and exponential function. A comparative study of thermoelastic analysis is given for material properties and disk thickness profiles. The results of are compared with those obtained by finite element method (FEM) that shows good agreement. The effect of thickness profiles, gradient parameters and angular velocity on the thermoelastic performance of the disk have been studied.

Keywords: Rotating disk, Variable thickness, Thermoelastic, Functionally graded material (FGM).

1. INTRODUCTION

Rotating disks have been used in many practical engineering applications, such as steam rotors, gas turbine rotors, centrifugal compressors, flywheels, and so on. The disks are subjected to both centrifugal and thermal forces, so the materials are required to prevent heat from being transferred to the shaft and bearings while preventing the fracture caused by stresses. It is hard to satisfy the requirement or conventional materials.

Functionally graded materials (FGMs) are a new type of advanced composite materials. FGMs can be employed which are often designed to work in severe environment with enhanced thermal properties, fracture toughness, wear resistance, corrosion resistance, and so on. Researchers have studied the performance of FGM disks with its composition changing from the outer surface to the inner surface with different designed variations of properties [1-5].

From early analyses on disks, Tutuncu [6], determined the stresses and deformations resulting from centrifugal forces in rotating especially orthotropic circular plates. He employed the classical laminated plate theory in the analysis, and the results are presented in a manner which illustrates the effect of anisotropy. Based on the classic Lamé problem for a pressurized homogeneous isotropic disk, Horgan and Chan [7] presented the effects of material inhomogeneity on the response of linearly elastic isotropic hollow circular cylinders or disks under uniform internal or external pressure. Eraslan *et al.* [8], provided a closed form solution for the shafts and disks which are made of functionally graded (FG) materials with the distribution of power and parabolic. They presented a comprehensive parametric analysis of rotating variable thickness elasto-plastic annular disks with inner boundaries subject to pressure or mounted on rigid inclusion. Kordkheili and Naghdabadi [9], used a semi-analytical approach to analyze axisymmetric thermoelastic deformations of hollow and solid rotating FG disks with the thermal and mechanical properties given by a power-law function of radii. Bayat *et al.* [10], analyzed FG rotating disks with variable thickness and presented an elastic solution, and the material properties and disk thickness profile are assumed as two power-law distributions. The effects of the material grading index and the geometry of the disk on the stresses and displacements have been investigated. Vullo and Vivio [11], developed a procedure for the evaluation of elastic stresses and strains in non-linear variable thickness rotating disks, either solid or annular, subjected to thermal load, having a fictitious density

* Corresponding author (m_zamani@yu.ac.ir ; m.zamani.n@gmail.com)

DOI : 10.1017/jmech.2015.95
Copyright © 2015 The Society of Theoretical and Applied Mechanics, R.O.C.
https://doi.org/10.1017/jmech.2015.95 Published online by Cambridge University Press

variation along the radius. Nejad *et al.* [12], obtained a complete three-dimensional set of field equations developed for elastic analysis of thick shells of revolution with arbitrary curvature and variable thickness along the meridional direction made of FGMs by using tensor analysis. Using plane elasticity theory and complementary functions method, Tutuncu and Temel [13], obtained axisymmetric displacements and stresses in functionally graded hollow cylinders, disks and spheres subjected to uniform internal pressure. Several thermoelastic analyses for FG rotating disks with variable thickness were investigated by Bayat *et al.* [14,15]. They employed a semi-analytical solution for the governing equation by dividing the disk into some virtual sub-domains, where property and thickness of the sub-domains were constant. Bayat *et al.* [16], presented an exact elastic solutions for axisymmetric variable-thickness hollow rotating discs with heat source made of FG materials under free-free and fixed-free boundary conditions. Nie and Batra [17], analyzed axisymmetric deformation of a rotating disk with its thickness, mass density, and thermal expansion coefficient and shear modulus varying in the radial direction. The disk was made of a rubber-like material that was modeled as an isotropic, linear thermoelastic and incompressible material. By introducing a semi-analytical three-dimensional elasticity solution, Asghari and Ghafoori [18], analyzed rotating FG disks for both hollow and solid disks. By assuming constant angular velocity around the central axis of disk, Long and Xian [19], also proposed an analytical solution to investigate steady thermal stresses in an FG circular annulus rotating disk. Based on the two dimensional thermo-elastic theories, Afsar and Go [20], focused on the finite element analysis of thermoelastic field in a thin circular FGM disk subjected to a thermal load and an inertia force due to rotation of the disk. Due to symmetry, the FGM disk assumed to have exponential variation of material properties in radial direction only. Zenkour and Mashat [21], provided the exact analytical and numerical solutions for a rotating variable-thickness annular disk. They considered inner and outer edges of the rotating variable-thickness annular disk to have free boundary conditions. An accurate and efficient solution procedure based on the elasticity theory was employed by Lotfian *et al.* [22], to investigate the elastic behavior of disks made of FG materials subjected to mechanical loads. Hasani *et al.* [23], obtained the distributions of stress and strain components of rotating disks with non-uniform thickness and material properties subjected to thermoelastic loading under different boundary conditions by semi-exact methods of Liao's homotopy analysis method, Adomian's decomposition method and He's variational iteration method. They assumed the distribution of temperature over the disk radius to have power forms with the higher temperature at the outer surface.

In recent years, by incorporating the variation of material properties into the discretization process, Gong *et al.* [24], have investigated a finite volume method for the steady thermoelastic analysis of the FGMs. Zafarmand and Hassani [25], obtained an elasticity solution for two-dimensional FG rotating annular and solid disks with variable thickness. Nejad *et al.* [26], provided a closed-form analytical solution based on the elasticity theory by assuming exponentially-varying properties in the radial direction and constant Poisson's ratio, for elastic analysis of disks made of FGMs subjected to internal and external pressure. Tutuncu and Temel [27], used the complementary functions method to develop an efficient unified method for thermoelastic analysis of FG rotating disks of variable thickness. They concluded that the closed-form solutions for thermoelastic analysis of variable thickness FG disks can be obtained only for specific forms of grading functions. Golmakani [28], conducted a large deflection thermoelastic analysis for FG solid and hollow rotating axisymmetric disks with uniform and variable thickness subjected to thermo-mechanical loading. The exact analytical solution of transient thermoelastic behaviors of rotating pressurized disks subjected to arbitrary boundary and initial conditions studied by Nejad and Afshin [29]. Assuming basic thermoelasticity theory under generalized assumptions, they analyzed the relations of temperature and transient thermal stresses in the radial direction by using the method of the separation of variables. Vullo *et al.* [30], investigated a theoretical method for the evaluation of elastic stresses and strains in rotating hyperbolic disks without singularity, also subjected to thermal load. They deduced the differential equation governing the radial displacement field of the hyperbolic disk from the governing equation of non-linearly variable thickness disks given by the power of a linear function of the radius. Nejad *et al.* [31] presented an exact closed-form analytical solution for elasto-plastic deformations and stresses in a rotating disk made of FGMs in which the elasto-perfectly-plastic material model is employed. In other work, Nejad *et al.* [32], presented an elastic parametric analysis for the purpose of investigating the limit angular speed, displacement and stresses in rotating disks made of FGMs based on Tresca yield criterion. As it is done in the works cited above, in such situations solution methods include integral transformations, development of finite element models, and, in some special cases, series solutions are attempted. Assuming the member is composed of many homogeneous layers of different properties emulating the FGM behavior is another way of tackling the problem on hand. In this work, two methods of analysis, namely, the analytical method and semi-analytical method of FG disk with variable thickness were used.

Although many earlier studies on rotating FG disks have considered different functions such as exponential or power for thickness and material distribution, to the best of the authors' knowledge, the effect of thickness and material function type on the displacement, stresses and temperature distribution in the disk with variable thickness due to general loading condition still remains under-researched. The present study deals with the Lame problem of disks with variable thickness composed of FGM subjected to body force (*e.g.* angular velocity), internal pressure (*e.g.* shrink fit pressure) and thermal loads (*e.g.* temperature gradient) (Fig. 1).

https://doi.org/10.1017/jmech.2015.95 Published online by Cambridge University Press

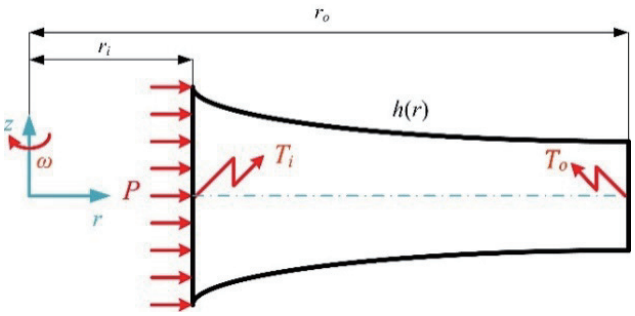


Fig. 1 Configuration and loading condition of disk with variable thickness.

Generally speaking, the variation of the property of the material in the FGM disks along the radial direction is assumed to be represented by the simple functions, such as power distribution and exponential distribution. The first function was the one introduced by Stodola [33], for variable thickness profile, defined by a power relationship given as a reference thickness multiplied by the variable raised to an exponent. This function does not allow defining profiles of solid disks. In the second type of functions, radial variations are assumed according to the exponential form. Obviously these functions are used for the simplicity of the equations, but for application purposes, they require a closer look. While in previous studies, a comparison between these two functions was not performed, here is focused on a method for comparing these functions. For this purpose, material properties such as modulus of elasticity, mass density, thermal expansion and the thermal conductivity are assumed to be represented by two law distributions along the radial direction. The Poisson's ratio will be assumed to be constant throughout. Three types of thickness profiles, namely uniform, exponential and hyperbolic are considered. The thickness of the disk is assumed to be sufficiently small compared with its outer diameter and also plane stress condition is invoked. The governing differential equation will be non-homogeneous with variable coefficients, which include material properties. It should be noted that while the governing displacement equation is homogeneous for a simple inner pressure case, it becomes non-homogeneous when the inertia force due to rotation and thermal loads are included. Analytical solutions are given according to different types of disks. In some cases, semi-analytical solutions for the temperature distribution and the displacement field are presented. The effect of geometry and material property on the radial displacement and stresses in FG rotating disks with variable thickness is investigated by studying their elastic behavior in four different cases. The governing second-order differential equation is derived and solved by analytical method.

2. GRADATION RELATION AND THICKNESS PROFILES

The thickness profile h of the disk is assumed to vary radially and is considered of the following two types

1. Power

$$h(r) = h_o\left(\frac{r}{r_o}\right)^{m_p}, \tag{1a}$$

2. Exponential

$$h(r) = h_o e^{m_e(r-r_o)}, \tag{1b}$$

where m_h and m_e are geometric parameters, and h_o is the thickness at the outer radius of the disk. To calculate the geometric parameters with respect to the thickness of the inner layer disk, the following equations can be used.

$$m_p = \frac{\ln(h_i / h_o)}{\ln(r_i / r_o)}, \tag{2a}$$

$$m_e = -\frac{\ln(h_i / h_o)}{r_o - r_i}, \tag{2b}$$

here h_i is the thickness at the inner radius of the disk. It is evident that the profile is convergent if $h_o / h_i > 1$ and it is divergent if $h_o / h_i < 1$. Different forms of the thickness profiles are shown in Fig. 2.

There are some models for expressing the variation of material properties in FGMs in the literature. The most commonly used of these models are given as the power-law and exponential distributions. In this study, the material property gradation through the disk radius is assumed to vary radially according to two different continuously nonlinear forms as follows

1. Power

$$\begin{cases} E(r) = E_0\left(\dfrac{r}{r_i}\right)^{n_p^1}, \quad \rho(r) = \rho_0\left(\dfrac{r}{r_i}\right)^{n_p^2}, \\ k(r) = k_0\left(\dfrac{r}{r_i}\right)^{n_p^3}, \quad \alpha(r) = \alpha_0\left(\dfrac{r}{r_i}\right)^{n_p^4}, \end{cases} \tag{3a}$$

2. Exponential

$$\begin{cases} E(r) = E_0 e^{n_e^1(r-r_i)}, \quad \rho(r) = \rho_0 e^{n_e^2(r-r_i)}, \\ k(r) = k_0 e^{n_e^3(r-r_i)}, \quad \alpha(r) = \alpha_0 e^{n_e^4(r-r_i)}, \end{cases} \tag{3b}$$

here n_p^i and n_e^i are grading indexes. As the inner surface of the FG disk consists of material A (P_A) and outer surface of material B (P_B), therefore the constants in Eq. (3) are determined as [18]

$$E_0 = E_A, \ \rho_0 = \rho_A, \ k_0 = k_A, \ \alpha_0 = \alpha_A, \tag{4a}$$

$$\begin{cases} n_p^1 = \dfrac{\ln(E_A / E_B)}{\ln(r_i / r_o)}, \ n_p^2 = \dfrac{\ln(\rho_A / \rho_B)}{\ln(r_i / r_o)}, \\ n_p^3 = \dfrac{\ln(k_A / k_B)}{\ln(r_i / r_o)}, \ n_p^4 = \dfrac{\ln(\alpha_A / \alpha_B)}{\ln(r_i / r_o)}, \end{cases} \tag{4b}$$

https://doi.org/10.1017/jmech.2015.95 Published online by Cambridge University Press

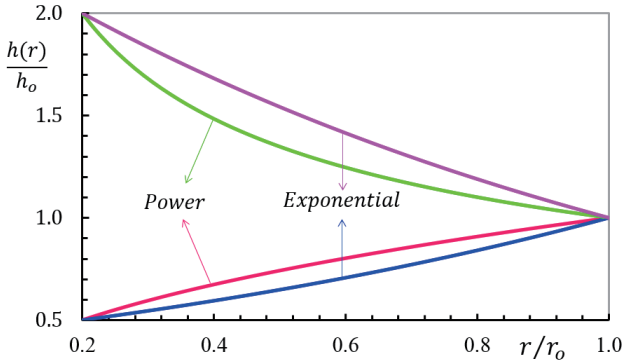


Fig. 2 Power and exponential thickness profiles for FG disk ($r_i / r_o = 0.2$).

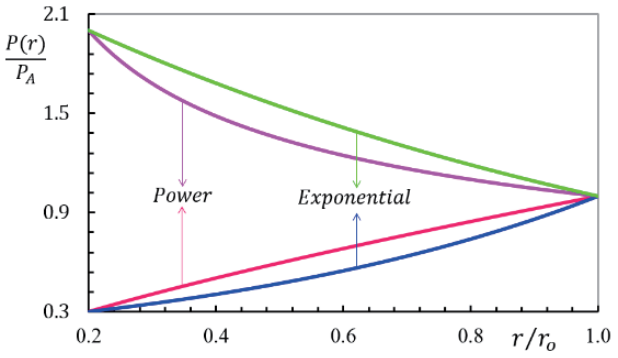


Fig. 3 Power and exponential FG functions for disk with variable thickness ($r_i / r_o = 0.2$).

$$\begin{cases} n_e^1 = \dfrac{\ln(E_A / E_B)}{r_i - r_o}, \quad n_e^2 = \dfrac{\ln(\rho_A / \rho_B)}{r_i - r_o}, \\ n_e^3 = \dfrac{\ln(k_A / k_B)}{r_i - r_o}, \quad n_e^4 = \dfrac{\ln(\alpha_A / \alpha_B)}{r_i - r_o}. \end{cases} \tag{4c}$$

For two types of gradient functions, dimensionless property along the radial direction is plotted in Fig. 3.

In this study it is assumed that the Poison's ratio is constant and the modulus of elasticity, thermal conductivity, thermal coefficient of expansion and density vary radially. It must be noted that the same grading index has been used in this study while defining the material properties for the modulus of elasticity, thermal conductivity, thermal coefficient and the density.

3. THEORETICAL FORMULATION AND EQUILIBRIUM EQUATIONS

3.1 Heat Conduction Equation

By consumption of an element in the cylindrical coordinate system in the steady state without internal heat source, according to the heat balance equation for steady-state heat conduction without heat generation, the Eq. (5) has been conducted

$$\frac{d}{dr}\left(k(r)h(r)\, r \frac{dT}{dr}\right) = 0 . \tag{5}$$

Solving the differential Eq. (5) finally the terms of temperature distribution $T(r)$ are conducted as follows

$$T(r) = c_1 \int_{r_i}^{r} \frac{dr}{rk(r)\, h(r)} + c_2 . \tag{6}$$

By exerting the boundary conditions for the temperature distribution

$$T(r) = T_i \left(1 - \frac{\int_{r_i}^{r} \dfrac{dr}{rh(r)k(r)}}{\int_{r_i}^{r_o} \dfrac{dr}{rh(r)k(r)}} \right) + T_o \left(\frac{\int_{r_i}^{r} \dfrac{dr}{rh(r)k(r)}}{\int_{r_i}^{r_o} \dfrac{dr}{rh(r)k(r)}} \right). \tag{7}$$

3.2 Equilibrium Equation

The plane elasticity theory (PET) or classical theory is based on the assumption that the straight lines perpendicular to the central axis of the cylinder remain unchanged after loading and deformation. According to this theory, the deformations are axisymmetric and do not change along the longitudinal cylinder. In other words, the elements do not have any rotation, and the shear strain and shear stress are assumed to be zero. Simplifying the radial equilibrium equation of the rotating disk with variable thickness for an infinitesimal element of the disk is conducted in the form below

$$\frac{1}{r}\left(\frac{\partial}{\partial r}\left(rh(r)\sigma_r\right)\right) - h(r)\frac{\sigma_\theta}{r} + rh(r)\rho(r)\,\omega^2 = 0 , \tag{8}$$

where $h(r)$ denotes thickness profile function, and ω stands for rotating angular velocity. Considering the existence of thermal loading and assuming the variation of the temperature gradient radially, thermal strain is the function of the radius as follows

$$\varepsilon^T = \alpha(r)\left(T(r) - T_{ref}\right) = \alpha(r)\Delta T(r) , \tag{9}$$

where $\Delta T(r)$ denotes the function of the gradient temperature distribution. In addition, the bases of constitutive equations for nonhomogeneous and isotropic materials in the plane stress state are as follows

$$\begin{Bmatrix} \sigma_r \\ \sigma_\theta \end{Bmatrix} = \frac{E(r)}{1-\nu^2}\begin{bmatrix} 1 & \nu \\ \nu & 1 \end{bmatrix}\begin{Bmatrix} \dfrac{du}{dr} \\ \dfrac{u}{r} \end{Bmatrix} - \frac{E(r)\,\alpha(r)\Delta T(r)}{1-\nu}, \tag{10}$$

https://doi.org/10.1017/jmech.2015.95 Published online by Cambridge University Press

where $E(r)$ and v denote modulus of elasticity and Poisson's ratio. By substituting Eq. (10) into Eq. (8) the result is

$$A_1\frac{d^2u}{dr^2}+A_2\frac{du}{dr}+A_3u+A_4=0\,, \tag{11}$$

were

$$\begin{cases} A_1=rh(r)E(r),\\ A_2=\dfrac{d}{dr}\big(rh(r)E(r)\big)\,,\\ A_3=-\dfrac{h(r)E(r)}{r}+\nu\dfrac{d}{dr}\big(h(r)E(r)\big)\,,\\ A_4=r(1+\nu)\Big\{(1-\nu)h(r)\rho(r)\,r\omega^2\\ \qquad -\dfrac{d}{dr}\big(h(r)E(r)\alpha(r)\Delta T(r)\big)\Big\}. \end{cases} \tag{12}$$

4. THERMOELASTIC SOLUTION

4.1 Case I: Power Profile & FG Power

Using power function for thickness profile and power function for material gradient, Eq. (7) can be determined as

$$\Delta T(r)=\frac{(T_o-T_i)\left(r^{-(m_p+n_p)}-r_i^{-(m_p+n_p)}\right)}{r_o^{-(m_p+n_p)}-r_i^{-(m_p+n_p)}}\,. \tag{13}$$

Substituting the terms (1a), (3a) and (13) into (11), the Navier equation is obtained as

$$\begin{aligned} &r^2\frac{d^2u}{dr^2}+(1+m_p+n_p)r\frac{du}{dr}+\big((n_p+m_p)\,\nu-1\big)\,u\\ &=\frac{\alpha_A(1+\nu)\,r^{n_p+2}}{r_i^{n_p}}\frac{d}{dr}\big(\Delta T(r)\big)-\frac{(1-\nu^2)\rho_A r^3\omega^2}{E_A}\\ &\quad+\frac{\alpha_A(1+\nu)(2n_p+m_p)\,r^{n_p+1}}{r_i^{n_p}}\Delta T(r)\,. \end{aligned} \tag{14}$$

The complete solution for u is the sum of general and particular solutions. Eq. (14) for the homogeneous case is the Euler-Cauchy's one. Putting the parameter r^λ instead of u, the characteristic equation is obtained

$$\lambda^2+(m_p+n_p)\lambda+\big((m_p+n_p)\,\nu-1\big)=0\,. \tag{15}$$

The roots of the above second-order polynomial equation are

$$\begin{cases} \lambda_1=\dfrac{-(m_p+n_p)+\sqrt{\Delta}}{2}\,,\ \lambda_2=\dfrac{-(m_p+n_p)-\sqrt{\Delta}}{2}\,,\\ \Delta=(m_p+n_p)^2-4(m_p+n_p)\,\nu+4\,. \end{cases} \tag{16}$$

Although the above equation has different roots for different quantities of Δ, because of the value of the Poisson's ratio which is in the range of 0 to 0.5, the term of Δ is always positive. As a result, the parameters λ_i always have the real values. So the homogenous solution of the Eq. (14) is obtained

$$u^h=C_1r^{\lambda_1}+C_2r^{\lambda_2} \tag{17}$$

Using the homogenous solution by Lagrange method, the particular solution can be derived in the following terms

$$u^P=\vartheta_1(r)\,r^{\lambda_1}+\vartheta_2(r)\,r^{\lambda_2} \tag{18}$$

After solving the set of Lagrange equations and integrating the terms $\vartheta_1(r)$ and $\vartheta_2(r)$, by substituting these two terms in Eq. (18), u^P is obtained as

$$\begin{aligned} u^P=&\frac{(T_o-T_i)(1+\nu)\,\alpha_A}{r_o^{-(m_p+n_p)}-r_i^{-(m_p+n_p)}}\times\\ &\left\{\left(\frac{n_p r_i^{-n_p}}{n_p(m_p-1-\nu)+m_p(\nu-1)}\right)r^{1-m_p}\right.\\ &\left.-\left(\frac{(2n_p+m_p)\,r_i^{-(2n_p+m_p)}}{2n_p^{\,2}+n_p(3+\nu+m_p)+m_p(1+\nu)}\right)r^{1+n_p}\right\}. \end{aligned} \tag{19}$$

Considering the Eqs. (16) ~ (18), the thermoelastic solution of the rotary FG variable thickness disk has been conducted

$$\begin{aligned} u=&C_1r^{\frac{1}{2}\left(-(m_p+n_p)+\sqrt{(m_p+n_p)^2-4(m_p+n_p)\,\nu+4}\right)}\\ &+C_2r^{\frac{1}{2}\left(-(m_p+n_p)-\sqrt{(m_p+n_p)^2-4(m_p+n_p)\,\nu+4}\right)}\\ &+\frac{(\nu^2-1)\rho_A\,\omega^2r^3}{\big(8+(3+\nu)(m_p+n_p)\big)E_A}\\ &+\frac{(T_o-T_i)(1+\nu)\,\alpha_A}{r_o^{-(m_p+n_p)}-r_i^{-(m_p+n_p)}}\\ &\times\left(\frac{n_p r_i^{-n_p}}{n_p(m_p-1-\nu)+m_p(\nu-1)}\right)r^{1-m_p}\\ &-\frac{(T_o-T_i)(1+\nu)\,\alpha_A}{r_o^{-(m_p+n_p)}-r_i^{-(m_p+n_p)}}\\ &\times\left(\frac{(2n_p+m_p)\,r_i^{-(2n_p+m_p)}}{2n_p^2+n_p(3+\nu+m_p)+m_p(1+\nu)}\right)r^{n_p+1}\,. \end{aligned} \tag{20}$$

Mechanical boundary conditions include internal pressure P at the inner surface. By applying boundary conditions, two unknown constants of C_1 and C_2 are calculated, as follows:

https://doi.org/10.1017/jmech.2015.95 Published online by Cambridge University Press

$$C_1=\frac{r_o r_i}{(\lambda_1+\nu)(r_o^{\lambda_2}r_i^{\lambda_1}-r_o^{\lambda_1}r_i^{\lambda_2})}\times\Big\{r_i^{\lambda_2-1}\Big[(3+\nu)\Psi_1 r_o^{\,2}+\Psi_2(1+\nu+n_p)\,r_o^{\,n_p}-(1-m_p+\nu)\,\Psi_3 r_o^{\,-m_h}-\alpha_A(1+\nu)\left(\frac{r_o}{r_i}\right)^{n_p}(T_o-T_i)\Big]-r_o^{\lambda_2-1}\Big[\frac{P(1-\nu^2)}{E_A}+\Psi_2(1+\nu+n_p)\,r_i^{\,n_p}+(3+\nu)\,\Psi_1 r_i^{\,2}-(1-m_p+\nu)\,\Psi_3 r_i^{\,-m_h}\Big]\Big\}, \tag{21a}$$

$$C_2=\frac{r_o r_i}{(\lambda_2+\nu)(r_o^{\lambda_2}r_i^{\lambda_1}-r_o^{\lambda_1}r_i^{\lambda_2})}\times\Big\{r_o^{\lambda_1-1}\Big[\frac{P(1-\nu^2)}{E_A}+(3+\nu)\,\Psi_1 r_i^{\,2}+\Psi_2(1+\nu+n_p)\,r_i^{\,n_p}-(1-m_p+\nu)\Psi_3 r_i^{\,-m_p}\Big]-r_i^{\lambda_1-1}\Big[(3+\nu)\,\Psi_1 r_o^{\,2}-\alpha_A(1+\nu+n_p)\left(\frac{r_o}{r_i}\right)^{n_p}(T_o-T_i)+\Psi_2(1+\nu+n_p)\,r_o^{\,n_p}-(1-m_p+\nu)\,\Psi_3 r_o^{\,-m_p}\Big]\Big\}, \tag{21b}$$

where

$$\begin{cases}\lambda_{1,2}=\dfrac{1}{2}\left(\pm\sqrt{(m_p+n_p)^2-4(m_p+n_p)\,\nu+4}\right)-\dfrac{(m_p+n_p)}{2},\\ \Psi_1=\dfrac{(\nu^2-1)\rho_A\omega^2}{\left(8+(3+\nu)(m_p+n_p)\right)E_A},\\ \Psi_2=-\dfrac{(T_o-T_i)(1+\nu)\,\alpha_A}{r_o^{-(m_p+n_p)}-r_i^{-(m_p+n_p)}}\left(\dfrac{(2n_p+m_p)r_i^{-(2n_p+m_p)}}{2n_p^{\,2}+n_p(3+\nu+m_p)+m_p(1+\nu)}\right),\\ \Psi_3=\dfrac{(T_o-T_i)(1+\nu)\,\alpha_A}{r_o^{-(m_p+n_p)}-r_i^{-(m_p+n_p)}}\left(\dfrac{n_p r_i^{-n_p}}{n_p(m_p-1-\nu)+m_p(\nu-1)}\right).\end{cases} \tag{22}$$

4.2 Case II: Power Profile & FG Exponential

Substitution of Eqs. (1a) and (3b) in Eq. (5) and then simplifying, the temperature differential equation is determined as:

$$r\frac{d^2T}{dr^2}+\left[\bar{n}r+(m_p+1)\right]\frac{dT}{dr}=0\,,\quad \bar{n}=\frac{n_e}{r_i}. \tag{23}$$

A closed-form solution of Eq. (23) seems to be extremely difficult if not impossible to obtain. Hence, in this section a semi-analytical method for the solution of Eq. (23) is attempted. In this method, the disk with variable thickness is divided into some disk layers with constant thickness. In addition, the FG disk is divided into some homogeneous disk layers along the gradient direction of the properties (Fig. 4).

Therefore, the governing equations convert to an ordinary differential equation with constant coefficients, which are assumed to be valid in k^{th} layer. That is

$$r^{[k]}\frac{d^2T}{dr^2}+\left[\bar{n}r^{[k]}+(m_h+1)\right]\frac{dT}{dr}=0\,. \tag{24}$$

Equation (24) is a homogeneous differential equation with constant variable. The general solution of Eq. (16) can be written as

$$T^{[k]}=D_1^{[k]}+D_2^{[k]}e^{\left[\frac{\bar{n}r^{[k]}+(m_p+1)}{r^{[k]}}\right]r}. \tag{25}$$

where $D_1^{[k]}$ and $D_2^{[k]}$ are unknown constants for k^{th} division. These unknowns are determined by applying the necessary boundary conditions between each of the two adjacent layers. The continuity of the temperature and its gradient are imposed at the interfaces of the adjacent layers. These continuity conditions at the interfaces are:

$$\Delta T(r)^{[k]}\Big|_{r=\frac{r^{[k]}+r^{[k+1]}}{2}}=\Delta T(r)^{[k+1]}\Big|_{r=\frac{r^{[k]}+r^{[k+1]}}{2}},\qquad \left[\frac{d\Delta T(r)}{dr}\right]^{[k]}\Big|_{r=\frac{r^{[k]}+r^{[k+1]}}{2}}=\left[\frac{d\Delta T(r)}{dr}\right]^{[k+1]}\Big|_{r=\frac{r^{[k]}+r^{[k+1]}}{2}}. \tag{26}$$

Given the continuity conditions, two equations are obtained. In general, if the disk is divided into N disk sub-domains, $2(N-1)$ equations are obtained. Using the two equations of boundary condition, $2N$ equations are obtained. The solution of these equations yields $2N$ unknown constants. Substitution of Eq. (25) in Eq. (11) generates the following governing equation for each sub-domain:

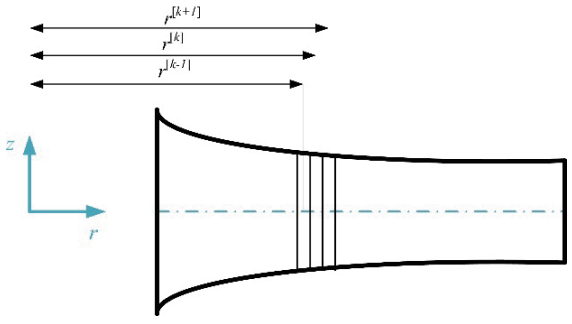


Fig. 4 Dividing disk with variable thickness into some disk layers with constant thickness.

https://doi.org/10.1017/jmech.2015.95 Published online by Cambridge University Press

$$A_1^{[k]}\frac{d^2u^{[k]}}{dr^2}+A_2^{[k]}\frac{du^{[k]}}{dr}+A_3^{[k]}u^{[k]}+A_4^{[k]}=0\,, \tag{27}$$

where

$$\begin{cases} A_1^{[k]}=(r^{[k]})^2\,,\\ A_2^{[k]}=(1+m_p+\overline{n}r^{[k]})r^{[k]}\,,\\ A_3^{[k]}=(\overline{n}r^{[k]}+m_p)\,\nu-1\,,\\ A_4^{[k]}=\dfrac{(1-\nu^2)\rho_A(r^{[k]})^3\,\omega^2}{E_A}\\ -\alpha_A(1+\nu)\,e^{\overline{n}(r^{[k]}-r_i)}\left(\dfrac{d(\Delta T)}{dr}\right)^{[k]}(r^{[k]})^2\\ -\alpha_A(1+\nu)\,\mathrm{r}^{[k]}\,e^{\overline{n}(r^{[k]}-r_i)}\left((2\overline{n}r^{[k]}+m_p)\,\Delta T^{[k]}\right). \end{cases} \tag{28}$$

The general solution of the homogeneous equation associated with Eq. (27) is

$$\begin{cases} \Delta^{[k]}=0\rightarrow\begin{cases} u^{[k]}=C_1^{[k]}e^{\lambda_1^{[k]}r}\\ +C_2^{[k]}re^{\lambda_1^{[k]}r}-\dfrac{A_4^{[k]}}{A_3^{[k]}}\,, \end{cases}\\ \Delta^{[k]}\neq0\rightarrow\begin{cases} u^{[k]}=C_1^{[k]}e^{\lambda_1^{[k]}r}\\ +C_2^{[k]}e^{\lambda_2^{[k]}r}-\dfrac{A_4^{[k]}}{A_3^{[k]}}\,, \end{cases} \end{cases} \tag{29}$$

where

$$\begin{cases} \lambda_{1,2}^{[k]}=\dfrac{-A_2^{[k]}\pm\sqrt{\Delta^{[k]}}}{2A_1^{[k]}}\,,\\ \Delta^{[k]}=(A_2^{[k]})^2-4A_1^{[k]}A_3^{[k]},\\ \dfrac{r^{[k]}-r^{[k+1]}}{2}<r<\dfrac{r^{[k]}+r^{[k+1]}}{2}\,. \end{cases} \tag{30}$$

4.3 Case III: Exponential Profile & FG Exponential

In this case, by substitution Eqs. (1b) and (3b) in Eq. (6), $T(r)$ is calculated as:

$$T(r)=\frac{c_1e^{r_i+r_o}}{k_Ah_o}\int_{r_i}^{r}\frac{dr}{re^{(m_e+n_e)r}}+c_2\,. \tag{31}$$

The solution of Eq. (31) is given as

$$\Delta T(r)=(T_o-T_i)\times\left(\frac{\zeta_1\left((m_e+n_e)r\right)-\zeta_1\left((m_e+n_e)r_i\right)}{\zeta_1\left((m_e+n_e)r_o\right)-\zeta_1\left((m_e+n_e)r_i\right)}\right). \tag{32}$$

with ξ_1 being the exponential integral defined by Abramowitz and Stegun [34]. Now inserting the above results back into Eq. (10) and after rearrangement,

$$\begin{cases} A_1^{[k]}=(r^{[k]})^2\,,\\ A_2^{[k]}=\left(1+(m_e+n_e)r^{[k]}\right)r^{[k]}\,,\\ A_3^{[k]}=(m_e+n_e)\,\nu r^{[k]}-1,\\ A_4^{[k]}=\dfrac{(1-\nu^2)\,\rho_A\omega^2(r^{[k]})^3}{E_A}\\ -\dfrac{\alpha_Ae^{\overline{n}r^{[k]}}(1+\nu)(2m_e+n_e)(T_o-T_i)(r^{[k]})^2}{\zeta_1\left((m_e+n_e)r_o\right)-\zeta_1\left((m+\overline{n})r_i\right)}\\ \times\left(\left(\zeta_1\left((m_e+n_e)\,r^{[k]}\right)-\zeta_1\left((m_e+n_e)\,r_i\right)\right)\right.\\ \left.-\dfrac{e^{-(m_e+n_e)r^{[k]}}}{(2m_e+n_e)\,r^{[k]}}\right). \end{cases} \tag{34}$$

Equation (33) is also solved using the same semi-analytical method as proposed in the previous section.

4.4 Case IV: Exponential Profile & FG Power

For power FG disks with exponential thickness profile, Eq. (27) can be determined as:

$$\begin{cases} A_1^{[k]}=(r^{[k]})^2\,,\\ A_2^{[k]}=(1+n_p+m_er^{[k]})r^{[k]}\,,\\ A_3^{[k]}=(m_er^{[k]}+n_p)\,\nu-1\,,\\ A_4^{[k]}=r^{[k]}(1+\nu)\left\{\dfrac{(1-\nu)\rho_o(r^{[k]})^2\,\omega^2}{E_o}\right.\\ -\alpha_o\left(\dfrac{r^{[k]}}{r_o}\right)^{n_p}\left(\left(\dfrac{d(\Delta T)}{dr}\right)^{[k]}r^{[k]}\right.\\ \left.\left.-\alpha_o\left(\dfrac{r^{[k]}}{r_o}\right)^{n_p}\left((2n_p+m_er^{[k]})\,\Delta T^{[k]}\right)\right\}, \end{cases} \tag{35}$$

where temperature distribution is given as follow

$$\Delta T^{[k]}=(D_1^{[k]}-T_{ref})+D_2^{[k]}e^{\left[\frac{m_er^{[k]}+(n_p+1)}{r^{[k]}}\right]r}\,, \tag{36}$$

$$\left(\frac{d(\Delta T)}{dr}\right)^{[k]}=D_2^{[k]}\left(\frac{m_er^{[k]}+(n_p+1)}{r^{[k]}}\right)\times e^{\left[\frac{m_er^{[k]}+(n_p+1)}{r^{[k]}}\right]r}. \tag{37}$$

The solution of Eq. (35) is obtained by Eq. (29).

5. RESULTS AND DISCUSSION

In this section, numerical calculations are carried out for specific cases. In order to show the effectiveness and accuracy of the approach suggested here, a comparison between responses of the present theories and those of finite element (FE) modeling can be performed.

https://doi.org/10.1017/jmech.2015.95 Published online by Cambridge University Press

A disk with variable thickness was modeled using ANSYS 2D simulations. The PLANE 223 element in axisymmetric mode, which is an element with eight nodes with up to four degrees of freedom per each node, was used for discretization. In order to model FG disk, an innovative application for multi-layering of thickness in the radial direction has been performed. Homogenous layers which are of identical thickness and step-variable elasticity modulus have been formed by this method. The disk with variable thickness consists of some coherent homogeneous layers whose properties at the contact location of the layers are the average of left and right limit of two layers boundaries. Internal pressures are applied to the nodes of inner layers. Considering the inertia force including angular velocity ω, the constant angular speed has been exerted to all nodes of the disk.

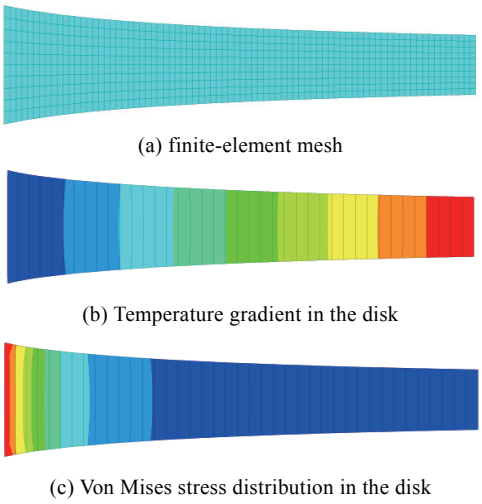
Figure 5 illustrates the finite-element mesh is established with ANSYS 2D. The analytical solution and FE analysis presented were applied to different cases with the characteristics listed in Table 1. The P_B/P_A value represents the ratio of the properties at the outer surface B and the inner surface A, which is assumed equal to 0.3 for all cases.

A FG disk with variable thickness subjected to internal pressure, uniform centrifugal force and thermal loading is considered. The applied internal pressure is $P_i = 40$MPa. The corresponding angular speed for a rotating FG annular disk is given as $\omega = 1000$rad/s and the surface temperature at the inner and outer surfaces is described as $T_i = 25$°C and $T_o = 100$°C, respectively.

In what follows, three numerical examples for the rotating FG disk with variable thickness will be introduced. The results are presented in a non-dimensional form so that absolute values of properties are unimportant. For numerical illustration of the elastic solutions of this study three examples are considered:

5.1 Example 1: Effect of Non-Homogenous Constant

In this section, numerical calculations are carried out for the specified case (Case III). Figures 6 ~ 8 show that this solution is in good agreement with verified FEM results. These plots demonstrate radial displacement, radial stress and circumferential stress for different values of n in the radial direction. Figure 6 shows the non-dimensional radial displacement along the radius for different values of the grading index n. It is observed that, the elasticity modulus increases with the increase in the power index n. Therefore, it could be seen that for higher values of n, radial displacement increases. In Fig. 7, the distribution of the radial stress along the radial direction for different values of n is shown. It is seen from the curves that at the same position $0 < r/r_o < 1$, for higher values of n, radial stress increases. Figure 8 shows the non-dimensional circumferential stresses for different values of the grading index n. As expected, the circumferential stress is the largest component of the stress which reaches its maximum value at inner surface. Besides, it could be seen that along the radial direction for all the magnitudes of n, the circumferential stress decreases.



(a) finite-element mesh

(b) Temperature gradient in the disk

(c) Von Mises stress distribution in the disk

Fig. 5 Finite-element model for the FG rotating disk with variable thickness (Case I).

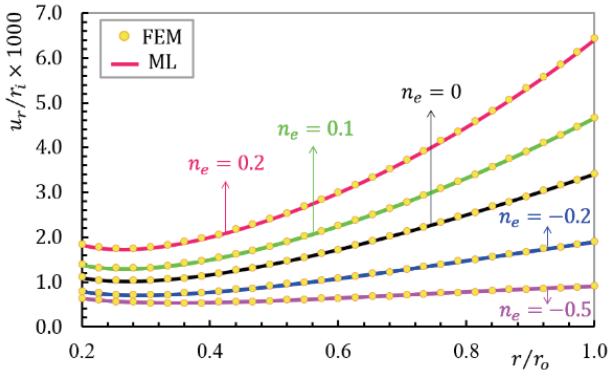


Fig. 6 Radial distribution of radial displacement ($h_i / h_o = 2$).

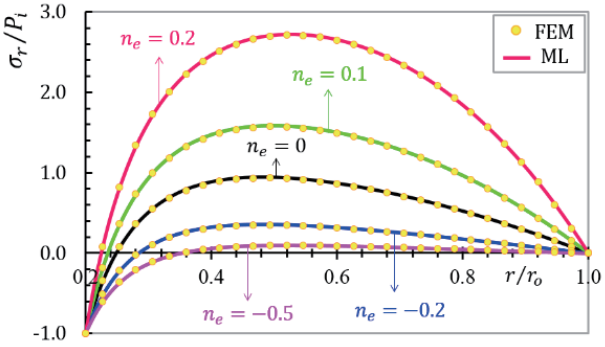


Fig. 7 Radial distribution of radial stress ($h_i / h_o = 2$).

Table 1 Characteristic parameters for the geometry and material properties.

Case No.	h_i (mm)	h_o (mm)	r_i (mm)	r_o (mm)	ν	E_A (GPa)	ρ_A (kg/m^3)	k_A (W/m°C)	α_A (10^{-6}/°C)	P_B/P_A
I	20	10	20	100	0.3	200	7800	20	12	0.3
II	20	10	20	100	0.3	200	7800	20	12	0.3
III	20	10	20	100	0.3	200	7800	20	12	0.3
IV	20	10	20	100	0.3	200	7800	20	12	0.3

https://doi.org/10.1017/jmech.2015.95 Published online by Cambridge University Press

5.2 Example 2: Effect of Angular Velocity

For the power profile and power FG case (Case I), one closed solution can be obtained for the FG disk with variable thickness under the general boundary condition.

Figure 9 illustrates a valid range for using disk layers in calculating the radial displacement and von Mises stress.

It could be observed that if the number of disk layers is more than 40 disks, there will be no significant effect on radial displacement. But the validity range of the von Mises stress is lesser than the radial displacement. In other words, one must analyse the disk with variable thickness using greater disk layer for determining von Mises stress. However, the error of using 80 disk layer in von Mises stress calculation is about 0.1%. In the all cases in question 80 disks are used.

The effects of angular velocity ω on the distribution of the stresses and radial displacement are presented in Figs. 10 ~ 12. The reported results are based on these parameters, $h_i / h_o = 2$, $P_A/P_B = 0.3$.

Figures 10 ~ 12 indicate that radial displacement and circumferential stress rise with increase in angular velocity. Also for the angular speed less than 500rad/s, the centrifugal force is less effective than internal pressure and thermal loading.

5.3 Example 3: Influence of Gradient Variation and Profile Functions

The influences of gradient variation and profile function on the distribution of displacement and stresses are examined in Figs. 13 ~ 15. All the results are calculated for a disk with constant geometrical parameters ($h_i / h_o = 2$) and constant gradient index ($P_A/P_B = 0.3$) under the same loading conditions.

Figures 13 ~ 15 show that changes in the material function have less dramatic effects on the radial and hoop stresses and radial displacement, as compared with those in the profile thickness, where this is seen more clearly in the radial displacement. In these plots, the results are presented under general loading but for closer look the results should be evaluated separately for each loading. In Table 2, the solution is completed by incorporating a certain set of sample disks. In order to elucidate the individual effect of each function on the equivalent stresses, two indexes are set to be fixed ($h_i / h_o = 2$, $P_A/P_B = 0.3$). For a better comparison between the results, the equivalent stress of each analysis to the maximum stress in a homogeneous disk with constant thickness (σ_0) has been normalized.

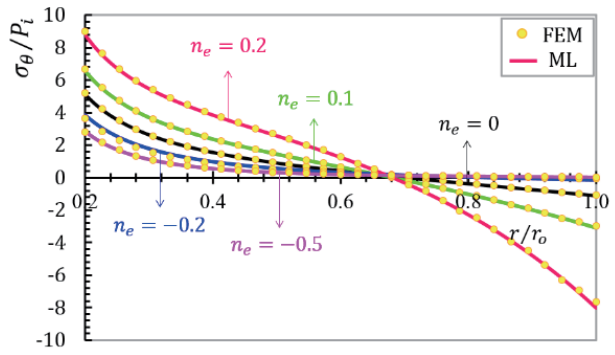


Fig. 8 Radial distribution of circumferential stress ($h_i / h_o = 2$).

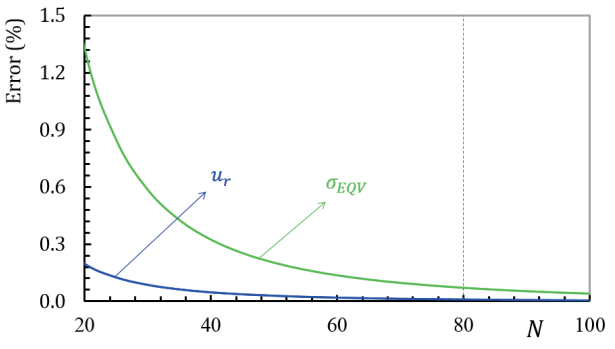


Fig. 9 Effect of the number of disk layers on the radial displacement and von Mises stress

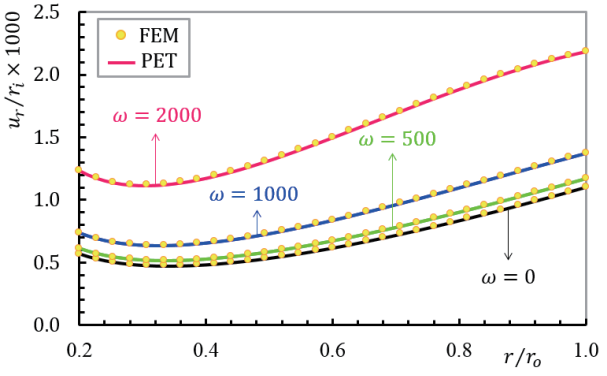


Fig. 10 Radial displacement subjected to various angular velocity ($h_i / h_o = 2$, $P_B/P_A = 0.3$).

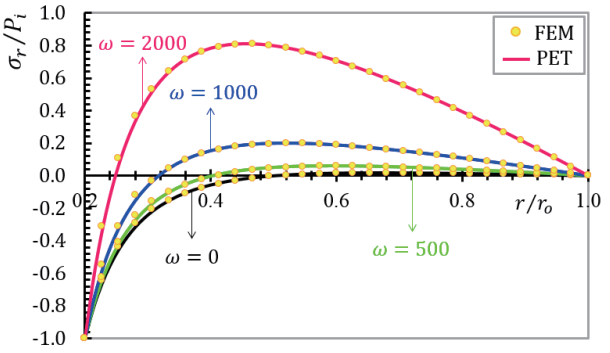


Fig. 11 Radial stress subjected to various angular velocity ($h_i / h_o = 2$, $P_B/P_A = 0.3$).

https://doi.org/10.1017/jmech.2015.95 Published online by Cambridge University Press

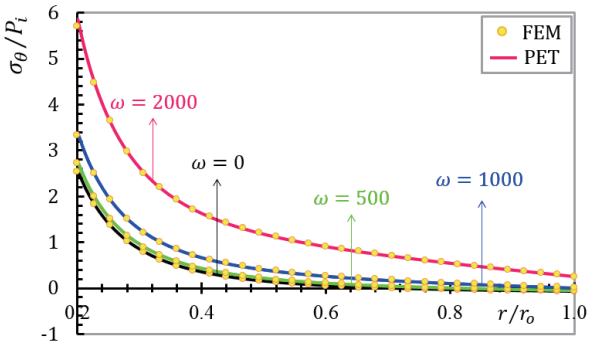


Fig. 12 Circumferential stress subjected to various angular velocity ($h_i / h_o = 2$, $P_B/P_A = 0.3$).

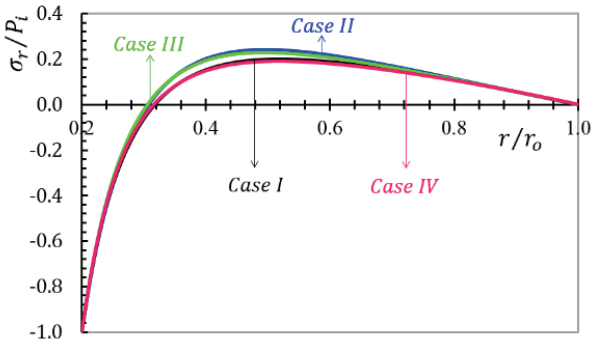


Fig. 14 Radial stress in the FG disk with variable thickness for different cases.

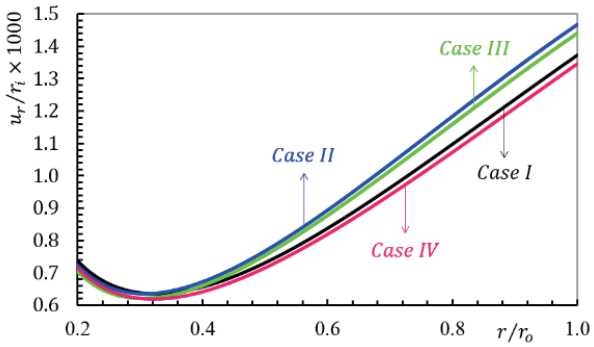


Fig. 13 Radial displacement in the FG disk with variable thickness for different cases.

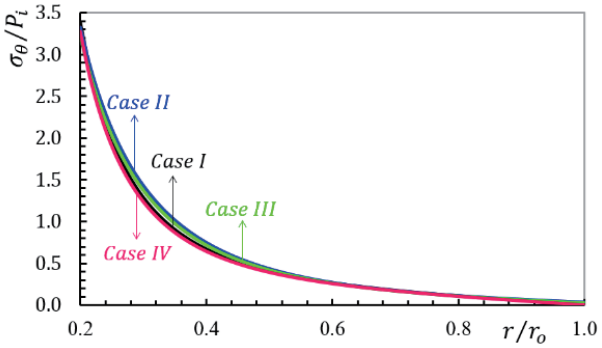


Fig. 15 Circumferential stress in the FG disk with variable thickness for different cases.

Table 2 Comparison of equivalent stress in the annular disks.

Thickness Profile	h_i / h_o	Material Type	P_A/P_B	Weight Ratio	$\frac{\sigma_{eq}\|_{thermal}}{\sigma_0}$	$\frac{\sigma_{eq}\|_{pressure}}{\sigma_0}$	$\frac{\sigma_{eq}\|_{rotation}}{\sigma_0}$
Uniform	1	Homogenous	1	1.000	1.000	1.000	1.000
Uniform	1	FG power	0.3	0.433	0.260	1.258	0.653
Uniform	1	FG exp.	0.3	0.505	0.319	1.151	0.669
Power	2	Homogenous	1	1.221	0.770	1.140	0.924
Exponential	2	Homogenous	1	1.332	0.783	1.086	0.792
Power	2	FG power	0.3	0.558	0.190	1.432	0.510
Exponential	2	FG power	0.3	0.611	0.199	1.367	0.524
Power	2	FG exp.	0.3	0.718	0.267	1.391	0.562
Exponential	2	FG exp.	0.3	0.654	0.243	1.249	0.539

In Table 2, it can be seen that the power FG disk with constant thickness has less weight than other disks. However, thermal stress is reduced to 74%; meanwhile, the stress resulting from internal pressure on the disk increases up to 25%. It can also be seen that in order to reduce the thermal stress and the stress subjected to centrifugal force on the disk, the power function is the best choice for profile thickness and material distribution. Another significant point is that the use of FG materials and disks with variable thickness increases the stress caused by internal pressure on the sample disks.

6. CONCLUSIONS

A general study of FG rotating disks with variable thickness is presented. Two common types of variation functions are used for profile and material function. Based on Navier thermoelastic equation, the governing equations of thick-walled disks are derived. Analytical and semi-analytical methods have been successfully employed to obtain the solution of elastic equation for both variable thickness and material rotating disks. The obtained results have been compared with the verified FEM solution. Good agreement was found

https://doi.org/10.1017/jmech.2015.95 Published online by Cambridge University Press

among the results. General observations of this study can be summarized as follows:

- Although closed-form analytic solutions have some advantages over other semi-analytical methods, semi-analytical method is in good agreement with FEM results.
- For the angular speed less than 500rad/s, the centrifugal force effect is negligible.
- Some parameters such as the index of gradient (n) and geometrical parameter (m) have also important effects on the results drawn.
- The thickening of the inner layer of a disk with variable thickness increases equivalent stress, which is due to the internal pressure.
- The solutions obtained show that the choice of an optimal function for material and thickness profile depends on the loading condition. For example, the power function is better than exponential function at the thermal and centrifugal loads conditions. However the exponential function is recommended for disks subjected to internal pressure.

REFERENCES

1. Gong, J. F., Ming, P. J., Xuan, L. K. and Zhang, W. P., "Thermoelastic Analysis of Three-Dimensional Functionally Graded Rotating Disks Based on Finite Volume Method," *Proceedings of The Institution of Mechanical Engineers Part C, Journal of Mechanical Engineering Science*, **228**, pp. 583–598 (2014).
2. Dai, H. L. and Zheng, H. Y., "Creep Buckling and Post-Buckling Analyses of a Viscoelastic FGM Cylindrical Shell with Initial Deflection Subjected to a Uniform In-Plane Load," *Journal of Mechanics*, **28**, pp. 391–399 (2012).
3. Nejad, M. Z., Hoseini, Z., Niknejad, A. and Ghannad, M., "Steady-State Creep Deformations and Stresses in FGM Rotating Thick Cylindrical Pressure Vessels," *Journal of Mechanics*, **31**, pp. 1–6 (2015).
4. Tokovyy, Y. V. and Ma, C. C., "Thermal Stresses in Anisotropic and Radially Inhomogeneous Annular Domains," *Journal of Thermal Stresses*, **31**, pp. 892–913 (2015).
5. Tokovyy, Y. V. and Ma, C. C., "Analytical Solutions to the Planar Non-Axisymmetric Elasticity and Thermoelasticity Problems for Homogeneous and Inhomogeneous Annular Domains," *International Journal of Engineering Science*, **47**, pp. 413–437 (2009).
6. Tutuncu, N., "Effect of Anisotropy on Stresses in Rotating Discs," *International Journal of Mechanical Sciences*, **37**, pp. 873–881 (1995).
7. Horgan, C. O. and Chan, A. M., "The Pressurized Hollow Cylinder or Disk Problem for Functionally Graded Isotropic Linearly Elastic Materials," *Journal of Elasticity*, **55**, pp. 43–59 (1999).
8. Eraslan, A. N. and Orcan, Y. A., "Parametric Analysis of Rotating Variable Thickness Elastoplastic Annular Disks Subjected to Pressurized and Radially Constrained Boundary Conditions," *Journal of Engineering and Environmental Sciences*, **28**, pp. 381–395 (2004).
9. Kordkheili, S. A. H. and Naghdabadi, R., "Thermoelastic Analysis of a Functionally Graded Rotating Disk," *Composite Structures*, **79**, pp. 508–516 (2007).
10. Bayat, M., Saleem, M., Sahari, B. B., Hamouda, A. M. S. and Mahdi, E., "Analysis of Functionally Graded Rotating Disks with Variable Thickness," *Mechanics Research Communications*, **35**, pp. 283–309 (2008).
11. Vullo, V. and Vivio, F., "Elastic Stress Analysis of Non-Linear Variable Thickness Rotating Disks Subjected to Thermal Load and Having Variable Density Along The Radius," *International Journal of Solids and Structures*, **45**, pp. 5337–5355 (2008).
12. Nejad, M. Z., Rahimi, G. H. and Ghannad, M., "Set of Field Equations for Thick Shell of Revolution Made of Functionally Graded Materials in Curvilinear Coordinate System," *Mechanika*, **3**, pp. 18–26 (2009).
13. Tutuncu, N. and Temel, B., "A Novel Approach to Stress Analysis of Pressurized FGM Cylinders, Disks and Spheres," *Composite Structures*, **91**, pp. 385–390 (2009).
14. Bayat, M., Saleem, M., Sahari, B. B., Hamouda, A. M. S. and Mahdi, E., "Mechanical and Thermal Stresses in a Functionally Graded Rotating Disk with Variable Thickness Due to Radially Symmetry Loads," *International Journal of Pressure Vessels and Piping*, **86**, pp. 357–372 (2009).
15. Bayat, M., Saleem, M., Sahari, B. B., Hamouda, A. M. S. and Reddy, J. N., "Thermo Elastic Analysis of Functionally Graded Rotating Disks with Temperature-Dependent Material Properties: Uniform and Variable Thickness," *International Journal of Mechanics and Materials in Design*, **5**, pp. 263–279 (2009).
16. Bayat, M., Mohazzab, A. H., Sahari, B. B. and Saleem, M., "Exact Solution for Functionally Graded Variable-Thickness Rotating Disc with Heat Source," *Proceedings of the Institution of Mechanical Engineers-Part C, Journal of Mechanical Engineering Science*, **224**, pp. 2316–2331 (2010).
17. Nie, J. G. and Barata, R. C., "Stress Analysis and Material Tailoring in Isotropic Linear Thermoelastic Incompressible Functionally Graded Rotating Disks of Variable Thickness," *Composite Structures*, **92**, pp. 720–729 (2010).
18. Asghari, M. and Ghafoori, E. A., "Three-Dimensional Elasticity Solution for Functionally Graded Rotating Disks," *Composite Structures*, **92**, pp. 1092–1099 (2010).
19. Long, X. P. and Xian, L. F., "Thermal Stress in Rotating Functionally Graded Hollow Circular Disks," *Composite Structures*, **92**, pp. 1896–1904 (2010).
20. Afsar, A. M. and Go, J. "Finite Element Analysis of Thermoelastic Field in a Rotating FGM Circular Disk," *Applied Mathematical Modelling*, **34**, pp. 3309–3320 (2010).

https://doi.org/10.1017/jmech.2015.95 Published online by Cambridge University Press

21. Zenkour, A. M. and Mashat, D. S., "Stress Function of a Rotating Variable-Thickness Annular Disk Using Exact and Numerical Methods," *Engineering*, **3**, pp. 422–430 (2011).
22. Lotfian, M. H., Nejad, M. Z., Abedi, M. and Ghannad, M., "An Elasticity Solution for Functionally Graded Hollow Disks under Radially Symmetry Loads," *Journal of Basic and Applied Scientific Research*, **11**, pp. 2435–2441 (2011).
23. Hassani, A., Hojjati, M. H., Farrahi, G. and Alashti, R. A., "Semi-Exact Elastic Solutions for Thermo-Mechanical Analysis of Functionally Graded Rotating Disks," *Composite Structures*, **93**, pp. 3239–3251 (2011).
24. Gong, J. F., Ming, P. J., Xuan, L. K. and Zhang, W. P., "Thermoelastic Analysis of Three-Dimensional Functionally Graded Rotating Disks Based on Finite Volume Method," *Proceedings of the Institution of Mechanical Engineers Part C*, *Journal of Mechanical Engineering Science*, **228**, pp. 583–598 (2014).
25. Zafarmand, H. and Hassani, B., "Analysis of Two-Dimensional Functionally Graded Rotating Thick Disks with Variable Thickness," *Acta Mechanics*, **225**, pp. 453–464 (2013).
26. Nejad, M. Z., Abedi, M., Lotfian, M. H. and Ghannad, M., "Elastic Analysis of Exponential FGM Disks Subjected to Internal and External Pressure," *Central European Journal of Engineering*, **3**, pp. 459–465 (2013).
27. Tutuncu, N. and Temel, B., "An Efficient Unified Method for Thermoelastic Analysis of Functionally Graded Rotating Disks of Variable Thickness," *Mechanics of Advanced Materials and Structures*, **20**, pp. 38–46 (2013).
28. Golmakani, M. E., "Large Deflection Thermoelastic Analysis of Shear Deformable Functionally Graded Variable Thickness Rotating Disk," *Composite Part B - Engineering*, **45**, pp. 1143–1155 (2013).
29. Nejad, M. Z. and Afshin, A., "Transient Thermoelastic Analysis of Pressurized Rotating Disks Subjected to Arbitrary Boundary and Initial Conditions," *Chinese Journal of Engineering*, Article ID 894902 (2014).
30. Vullo, V., Vivio, F. and Cifani, P., "Theoretical Stress Analysis of Rotating Hyperbolic Disk without Singularities Subjected to Thermal Load," *Journal of Thermal Stress*, **37**, pp. 117–136 (2014).
31. Nejad, M. Z., Rastgoo, A. and Hadi, A., "Exact Elasto-Plastic Analysis of Rotating Disks Made of Functionally Graded Materials," *International Journal of Engineering Sciences*, **85**, pp. 47–57 (2014).
32. Nejad, M. Z., Rastgoo, A. and Hadi, A., "Onset Yield Analysis of Rotating Disks Made of Functionally Graded Materials Using Tresca Yield Criterion," *Modares Mechanical Engineering*, **14**, pp. 68–74 (2014) (in Persian).
33. Stodola, A., *Dampf und Gasturbinen*, 6th Ed., Springer, Berlin Heidelberg (1924).
34. Abramowitz, M. and Stegun, I. A., *Handbook of Mathematical Functions*, Dover Publications, New York (1965).

(Manuscript received January 23, 2014,
accepted for publication August 23, 2015.)

https://doi.org/10.1017/jmech.2015.95 Published online by Cambridge University Press